

[CASE REPORT]

Osteoclast-like Giant Cell-type Pancreatic Anaplastic Carcinoma Presenting with a Duodenal Polypoid Lesion

Hiroyuki Matsubayashi¹, Junichi Kaneko¹, Junya Sato¹, Tatsunori Satoh¹,
Hirotoshi Ishiwatari¹, Teichi Sugiura², Ryo Ashida², Katsuhiko Uesaka²,
Keiko Sasaki³ and Hiroyuki Ono¹

Abstract:

Osteoclast-like giant cell-type (OCGC) anaplastic carcinoma is a rare variant of pancreatic ductal adenocarcinoma, and its imaging characteristics and progression pattern have not been fully clarified. The patient was a 73-year-old man who had been incidentally found to have a pancreatic head tumor. Computed tomography demonstrated a 3-cm marginally enhanced mass at the pancreatic head, continuing toward the duodenum. Diffusion-weighted magnetic resonance imaging showed a retained diffusion capacity. Duodenoscopy revealed a 1.5-cm polypoid lesion, covered by a dirty coat, near the major papilla. Surgical material revealed OCGC pancreatic anaplastic carcinoma protruding to the duodenum, accompanied by multiple hemorrhagic foci and hemosiderin precipitations.

Key words: pancreas, duodenum, anaplastic carcinoma, osteoclast-like giant cell, hemorrhaging

(Intern Med 58: 3545-3550, 2019)

(DOI: 10.2169/internalmedicine.3271-19)

Introduction

Anaplastic carcinoma is a rare undifferentiated variant accounting for only 0.08% of total pancreatic cancers, 0.5% (1) of resected pancreatic cancers, and 1.4% (2) of resected pancreatic ductal adenocarcinoma (PDAC). Pancreatic anaplastic carcinoma (PAC) shows oncogenic molecular alterations similar to those of PDAC (i.e. activation of *K-ras* oncogene and inactivation of suppressor genes, including *CDKN2A/p16*, *TP53*, and *DPC4*) (3) and is thought to represent a subtype of PDAC. PAC is thought to show an aggressive biological behavior; however, the patient survival can be significantly improved by surgical resection (4) or depending on the presence of osteoclast-like giant cells (OCGCs) (5) and the purity of OCGCs (i.e., no epithelial neoplasm) (3).

However, studies showing clinical images and the progression pattern of PAC have been lacking. We herein report a case of OCGC-type PAC that presented with a protruding

duodenal mass and developing pancreatitis, which enabled us to make a preoperative diagnosis.

Case Report

A 73-year-old man was referred to our hospital for the investigation of a mass lesion located at the pancreatic head. He had a history of diabetes, hyperlipidemia, and lung cancer (bronchioloalveolar carcinoma, 24 mm, pT1bN0M0, stage IA) at 71 years of age, for which he had undergone right-upper lobectomy and subsequent adjuvant chemotherapy with tegafur/uracil. His blood tests showed slight anemia (hemoglobin: 12.9 g/dL, normal: 13.5-17.6 g/dL) and elevated levels of serum amylase (431 U/L, normal: 37-125 U/L), hemoglobin A1c (6.8%, normal: 4.3-5.8%), and cancer antigen 19-9 (CA19-9)(294 U/mL, normal: <37 U/mL). The current pancreatic mass had been incidentally detected by computed tomography (CT) conducted to follow his post-operative lung lesion. His family history was not notable.

Abdominal ultrasonography (Fig. 1) revealed an irregular-

¹Division of Endoscopy, Shizuoka Cancer Center, Japan, ²Division of Hepato-pancreaticobiliary Surgery, Shizuoka Cancer Center, Japan and ³Division of Pathology, Shizuoka Cancer Center, Japan

Received: April 29, 2019; Accepted: July 8, 2019; Advance Publication by J-STAGE: August 28, 2019

Correspondence to Dr. Hiroyuki Matsubayashi, h.matsubayashi@scchr.jp

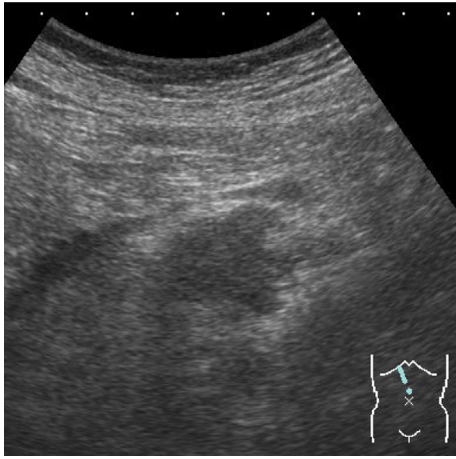


Figure 1. Abdominal ultrasonography (vertical scan). An irregular-margined low-echoic mass was seen at the pancreas head.

margined, low-echoic pancreatic mass, 30 mm in size. Enhanced CT (Fig. 2) demonstrated a heterogeneously ill-attenuated mass located at the pancreatic uncinate process and continuously protruding into the duodenum. The enhancement recovered slightly in the late phase, especially at the tumor margin. Only the peripancreatic lymph nodes were slightly swollen, they can thus be interpreted as either “inflammatory or non-cancerous” or “cancer metastasis-positive”. Magnetic resonance imaging (MRI) (Fig. 3) showed a low-signal-intensity lesion in both T1- and T2-weighted images. Diffusion-weighted imaging (DWI) showed a retained diffusing capacity at the lesion when compared with the surrounding pancreas.

During these imaging examinations, the patient complained of intermittent abdominal pain; this was suggestive of pancreatitis, based on the elevated level of serum amylase. Duodenoscopy (Fig. 4A) revealed an approximately 15-

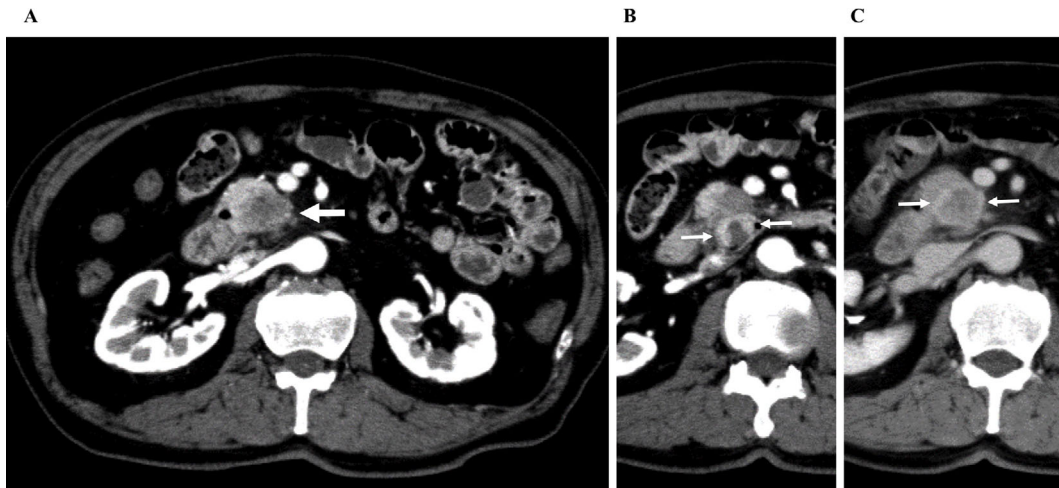


Figure 2. Enhanced computed tomography (CT). The arterial phase (47 seconds after contrast injection) of the CT image showed a low-attenuated mass located at the pancreatic uncinate process (arrow) (A) continuously invading the duodenum with marginal enhancement (small arrow) (B). The tumor was slightly enhanced at the late phase (3 minutes), especially at the margin (small arrows) (C).

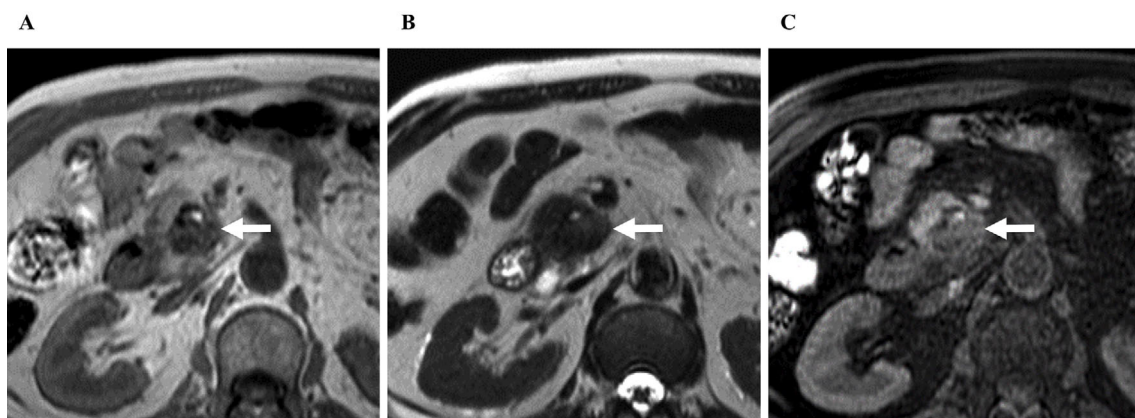


Figure 3. Magnetic resonance imaging (MRI). A low-signal-intensity mass was seen on T1-weighted (A), T2-weighted (B), and diffusion-weighted (C) images.

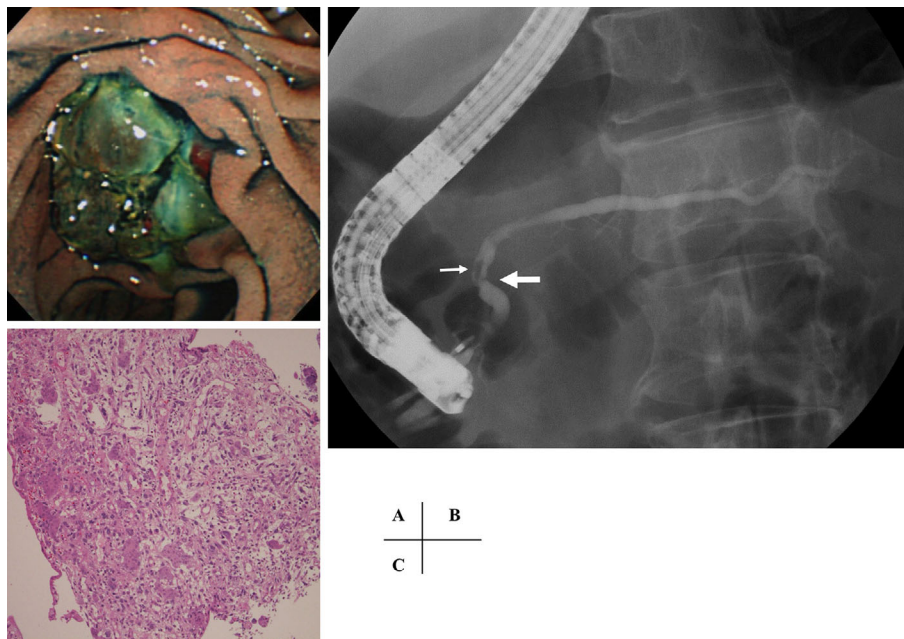


Figure 4. Endoscopic retrograde pancreatography. **A:** An indigocarmine-sprayed duodenoscopic view showed a protruding tumor, covered with a dirty coat, at the anal side of the major papilla. **B:** Pancreatography visualized faint stenosis of the main pancreatic duct (arrow) and a floating filling defect nearby (small arrow). **C:** A forceps biopsy specimen showed undifferentiated carcinoma with many osteoclast-like giant cells (Hematoxylin and Eosin staining, $\times 100$).

mm polypoid lesion, covered with a dirty coat, at the anal side of the major papilla. Endoscopic retrograde pancreatography demonstrated the irregularly narrowed main pancreatic duct (MPD) and a crumbling filling defect inside the MPD (Fig. 4B). Endoscopic naso-pancreatic duct drainage (ENPD) was performed to relieve pancreatitis. The patient's serum amylase level had normalized by the next day (76 U/L), and his abdominal pain had disappeared. Histology of the forceps biopsy specimen from the duodenal polyp revealed undifferentiated carcinoma with many OCGCs (Fig. 4C). Cytology of the pancreatic juice collected through the ENPD demonstrated cell clusters of adenocarcinoma. The patient underwent pancreaticoduodenectomy following the diagnosis of OCGC-type PAC [T3(Du)N0M0, stage IIA by both classifications of Japan Pancreas Society (JPS) (7th edition) and Union for International Cancer Control (UICC) (8th edition)].

A macroscopic view of the surgical material showed a heterogeneously hemorrhagic whitish mass (3 cm) and the continuing brownish tumor protruding into the duodenal lumen (2 cm) (Fig. 5A). The macroscopic brownish areas were microscopically hemorrhaging and hemosiderin precipitation (Fig. 5B). The tumor consisted mostly of undifferentiated carcinoma containing many OCGCs (Fig. 5C) and partially of well-differentiated adenocarcinoma (Fig. 5D). The pathological diagnosis was osteoclast-like giant cell-type anaplastic carcinoma of the pancreas. Cancer permeations into the lymph duct and peripheral vein were positive, and neural invasion was recognized. The two nearest lymph nodes were positive for carcinoma metastasis. Immunostain-

ing of CDKN2A/p16 was diffusely repressed, while that of TP53 diffusely overexpressed in the tumor cells. Cytokeratin AE1/AE3 and MUC1 were similarly positive in the differentiated adenocarcinoma components but negative in the dedifferentiated cancer cells. Immunostaining of CA19-9 and Vimentin was diffusely positive in the cancer cells. KP-1 was positive not only in the inflammatory cells but also in the cancer cells, including OCGCs. The Ki-67 labeling index was 42% as the average of 3 randomly chosen areas consisting of 500 cancer cells each (Fig. 5E-H).

The patient's postoperative course was uneventful, and he was discharged after two weeks. The patient was transferred to a local hospital and underwent adjuvant chemotherapy with gemcitabine. However, five months after the surgery, multiple liver metastases developed, and he ultimately succumbed in the eighth month due to cancer progression.

Discussion

PAC is a rare variant of pancreatic cancer, accounting for 1.4% (2) of resected PDAC. OCGC-type PAC is even rarer, accounting for only 0.2% of pathology-confirmed PDAC (5). Hoshimoto et al. analyzed 60 previously reported cases of Japanese PAC (mostly written in the Japanese language) and summarized the characteristics of these PAC cases. They presented a mean age of 61.5 years (range: 32 to 85 years), a slight male predominance (63%), main complaints of abdominal pain (48%) and back pain (17%), frequent elevation of serum CA19-9 (55%), almost equal distribution within the pancreas (head: 53%, body to tail: 42%,

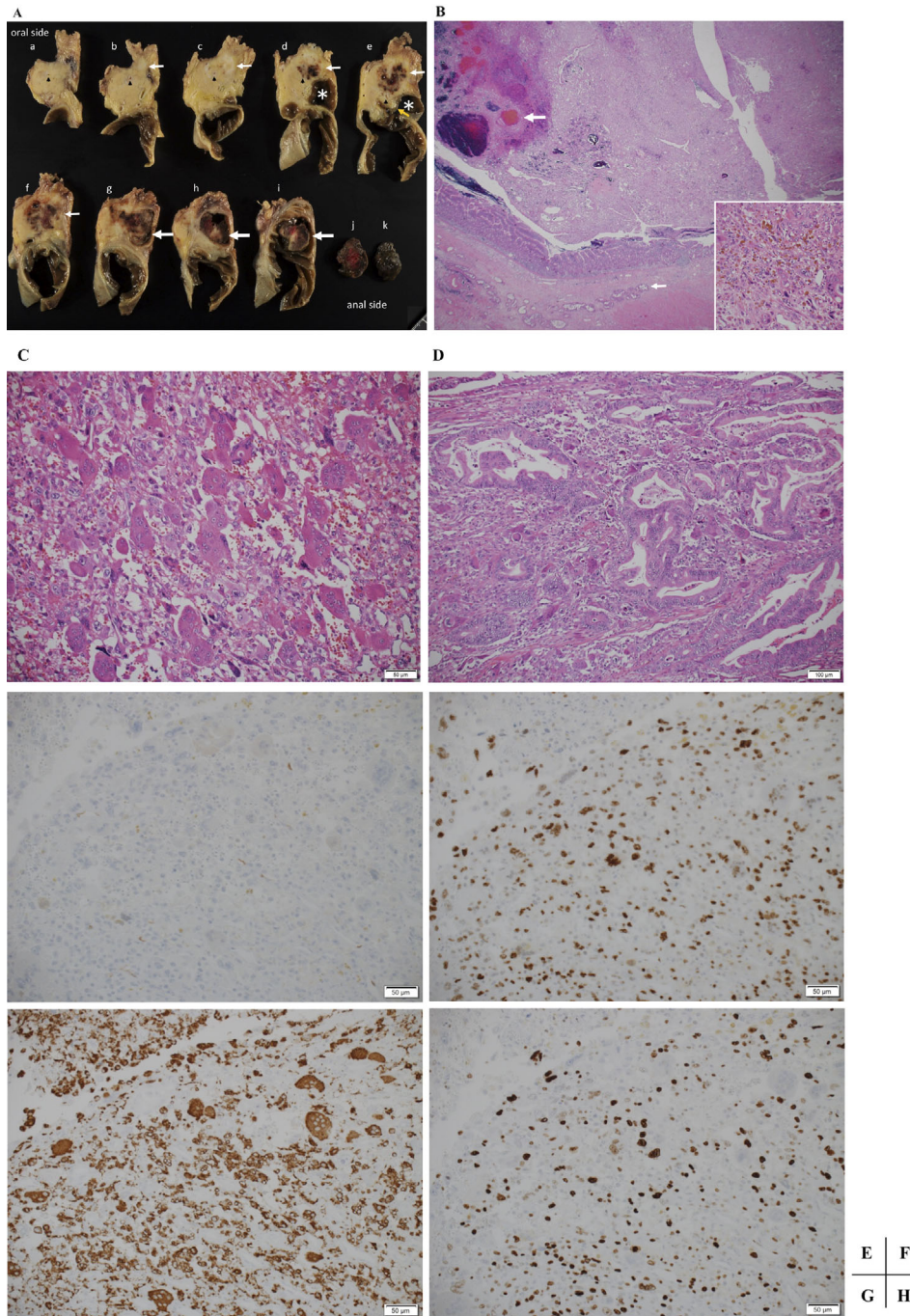


Figure 5. Pathological view of the resected specimen. A macroscopic view of the resected materials (A) showed a pancreatic tumor (small arrow) and tumor continuously protruding into the duodenum (arrow). The cut surface of the tumor was mostly accompanied by brownish areas or hemorrhaging. The main pancreatic duct (black arrowhead) was involved with the tumor at the marginal site. The major papilla (yellow arrow) was located at the margin of the duodenal diverticulum (asterisk). A low-power view of the protruding duodenal tumor and duodenal wall (B) showed hemorrhagic lesions (arrow) with hemosiderin precipitates [inset, Hematoxylin and Eosin (H&E) staining, $\times 100$] and adenocarcinoma invading the submucosa (small arrow) (H&E staining, $\times 12.5$). A high-power view of the tumor demonstrated many osteoclast-like giant cells within the undifferentiated carcinomas and red blood cells (C) (H&E staining, $\times 200$, a bar size: $50\ \mu\text{m}$) and a well-differentiated adenocarcinoma component (D) (H&E staining, $\times 100$, a bar size: $100\ \mu\text{m}$). Immunostaining of CDKN2A/p16 was diffusely repressed (E) ($\times 200$), whereas that of TP53 was overexpressed in the cancer cells (F) ($\times 200$). The KP-1 protein expression was positive not only in the inflammatory cells but also in the cancer cells, including the osteoclast-like giant cell-type anaplastic carcinoma cells (G) ($\times 200$). The Ki-67 labeling index was 42% in the randomly selected area (H) ($\times 200$).

and entire pancreas: 5%), and a median size of 6 cm (range: 1.5 to 24 cm) (6).

Little is known about the imaging features and progression patterns of this rare tumor type (7, 8). Fukukura et al. analyzed the CT and MRI scans of seven cases of OCGC-type PAC and reported several findings: a smooth-margined low-attenuated mass on CT and a low signal intensity on T1-weighted, T2-weighted, and diffusion-weighted imaging, reflecting hemosiderin precipitates (7). Khashab et al. used endoscopic ultrasonography (EUS) to examine six cases of PAC; five cases were observed as heterogeneous low-echoic masses. Four of these six cases demonstrated PAC components in EUS-fine-needle aspiration (EUS-FNA) samples (9). In the current case, the imaging findings for CT, MRI, and ultrasonography were quite similar to those of the cases reported by Fukukura et al. (7). Multiple foci of hemosiderin precipitates were also recognized within the tumor, as reflected in the low signal intensity on all three MRI modalities (7).

Hoshimoto et al. reported that the macroscopic view of the resected materials of PAC often indicate intra-tumor hemorrhaging (77%) and sometimes cystic formation (33%) (6). These findings are suggestive of the natural course of tumor development causing hemorrhagic necrosis, as the hemorrhaging changes into a hemosiderin clot, while necrosis leads to cyst formation. In our case, we observed hemorrhaging and diffuse hemosiderin precipitates in both the pancreatic and duodenal lesions, but no prominent cystic changes were apparent, suggesting a relatively early stage of detection by postoperative screening. The viable interstitial and tumor cells predominantly seen at the marginal area were thought to be reflected as marginal enhancement on late-phase images (Fig. 2).

According to a report from the Mayo Clinic, the prognosis in cases of PAC is poor if the lesions cannot be treated with surgery [overall survival (OS): 34.1 months in resected cases vs. 3.3 months in non-resected cases, $p=0.001$] (4). When surgically resected, in a condition-matched comparison, patients had a survival similar to ordinary PDAC (44.1 vs. 39.9 months, $p=0.763$) (4). This trend was the same when analyzing the American National Cancer Data Base (NCDB); the post-surgery 5-year survival rate was 22% in the PAC group and 17% in the PDAC group ($p=0.32$) (1). However, comparison of PACs with and without OCGCs indicated that tumors with OCGCs portended a significantly better prognosis (5-year survival: 50% vs. 15%, $p < 0.001$) (1). Another clinicopathological study by Luchini et al. also showed that the post-operative OS was significantly better in patients with pure OCGC-PAC ($n=9$) than in those with OCGC-PAC with a PDAC component ($n=13$) (median OS: 36 months vs. 15 months, $p=0.04$) (3). The current case of OCGC-PAC was accompanied by an adenocarcinoma component (Fig. 5D) and showed aggressive progression resistant to adjuvant chemotherapy with gemcitabine.

A recent European and American multicenter study demonstrated a significantly higher incidence of PD-L1 positiv-

ity in OCGC-type PACs (63%) than in ordinary PDACs ($p=0.04$) and a worse prognosis in OCGC-type PAC cases with PD-L1 expression than in those without (hazard ratio: 3.98, $p=0.12$) (10). However, in cases of non-small-cell lung cancers, immune-checkpoint inhibitors, such as pembrolizumab and atezolizumab, are more effective in PD-L1-positive cases (11, 12). In the future, we need to keep these data in mind when treating patients with OCGC-type PACs.

In conclusion, we encountered a case of osteoclast-like giant cell-type pancreatic anaplastic carcinoma forming a duodenal protruding mass and causing pancreatitis. A relatively smooth demarcation of the tumor margin, ill (or marginal) enhancement, intra-tumorous hemorrhaging, and hemosiderin precipitation were viewed as characteristic findings of this tumor.

The authors state that they have no Conflict of Interest (COI).

References

1. Paniccia A, Hosokawa PW, Schulick RD, et al. A matched-cohort analysis of 192 pancreatic anaplastic carcinomas and 960 pancreatic adenocarcinomas: A 13-year North American experience using the National Cancer Data Base (NCDB). *Surgery* **160**: 281-292, 2016.
2. Muraki T, Reid MD, Basturk O, et al. Undifferentiated carcinoma with osteoclastic giant cells of the pancreas: clinicopathologic analysis of 38 cases highlights a more protracted clinical course than currently appreciated. *Am J Surg Pathol* **40**: 1203-1216, 2016.
3. Luchini C, Pea A, Lionheart G, et al. Pancreatic undifferentiated carcinoma with osteoclast-like giant cells is genetically similar to, but clinically distinct from, conventional ductal adenocarcinoma. *J Pathol* **243**: 148-154, 2017.
4. Clark CJ, Arun JS, Graham RP, et al. Clinical characteristics and overall survival in patients with anaplastic pancreatic cancer. *Am Surg* **80**: 117-123, 2014.
5. Clark CJ, Graham RP, Arun JS, et al. Clinical outcomes for anaplastic pancreatic cancer: a population-based study. *J Am Coll Surg* **215**: 627-634, 2012.
6. Hoshimoto S, Matsui J, Miyata R, et al. Anaplastic carcinoma of the pancreas: case report and literature review of reported cases in Japan. *World J Gastroenterol* **22**: 8631-8637, 2016.
7. Fukukura Y, Kumagai Y, Hirahara M, et al. CT and MRI features of undifferentiated carcinomas with osteoclast-like giant cells of the pancreas: a case series. *Abdom Radiol (NY)* **44**: 1246-1255, 2019.
8. Yang KY, Choi JI, Choi MH, et al. Magnetic resonance imaging findings of undifferentiated carcinoma with osteoclast-like giant cells of pancreas. *Clin Imaging* **40**: 148-151, 2016.
9. Khashab MA, Emerson RE, DeWitt JM. Endoscopic ultrasound-guided fine-needle aspiration for the diagnosis of anaplastic pancreatic carcinoma: a single-center experience. *Pancreas* **39**: 88-91, 2010.
10. Luchini C, Cros J, Pea A, et al. PD-1, PD-L1, and CD163 in pancreatic undifferentiated carcinoma with osteoclast-like giant cells: expression patterns and clinical implications. *Hum Pathol* **81**: 157-165, 2018.
11. Herbst RS, Baas P, Kim DW, et al. Pembrolizumab versus docetaxel for previously treated, PD-L1-positive, advanced non-small-cell lung cancer (KEYNOTE-010): a randomised controlled trial. *Lancet* **387**: 1540-1550, 2016.

12. Rittmeyer A, Barlesi F, Waterkamp D, et al. Atezolizumab versus docetaxel in patients with previously treated non-small-cell lung cancer (OAK): a phase 3, open-label, multicentre randomised controlled trial. *Lancet* **389**: 255-265, 2017.

The Internal Medicine is an Open Access journal distributed under the Creative Commons Attribution-NonCommercial-NoDerivatives 4.0 International License. To view the details of this license, please visit (<https://creativecommons.org/licenses/by-nc-nd/4.0/>).

© 2019 The Japanese Society of Internal Medicine
Intern Med 58: 3545-3550, 2019